

## Neutrino Oscillation Results from the Liquid Scintillator Neutrino Detector

W. C. Louis, R. L. Burman,  
F. J. Federspiel, G. T. Garvey,  
G. B. Mills, V. Sandberg, R. Tayloe,  
D. H. White (P-25),  
J. B. Donahue (LANSCE-7),  
collaborators from  
University of California at Riverside,  
University of California at San Diego,  
University of California at Santa  
Barbara,  
Embry-Riddle Aeronautical University,  
University of California Intercampus  
Institute for Research at Particle  
Accelerators,  
Linfield College,  
Louisiana State University,  
Louisiana Tech University,  
University of New Mexico,  
Southern University,  
and Temple University

In the past few years, a number of experiments have searched for neutrino oscillations, in which a neutrino of one type (such as  $\bar{\nu}_\mu$ ) spontaneously transforms into a neutrino of another type (such as  $\bar{\nu}_e$ ). In the standard model of particle physics, neutrinos are considered to be massless, but the existence of neutrino oscillations would imply that neutrinos actually do have mass. Neutrino mass of even a few electronvolts would profoundly affect theories related to cosmology and to the development of structure in the universe.

In 1995 the LSND (Liquid Scintillator Neutrino Detector) collaboration published data showing candidate events that are consistent with  $\bar{\nu}_\mu \rightarrow \bar{\nu}_e$  oscillations.<sup>1</sup> Since then, the collaboration has reported additional data that provide stronger evidence for neutrino oscillations.<sup>2,3</sup> The LSND results complement hints from solar and atmospheric neutrino experiments that neutrino oscillations occur. In the solar experiments the sun emits fewer neutrinos than the standard solar model predicts, and in the atmospheric experiments the ratio of muon neutrinos to electron neutrinos that are generated by cosmic-ray interactions in the upper atmosphere is unexpectedly low. This current neutrino data combined with data from future experiments may eventually allow physicists to determine the masses and mixings of all three flavors of neutrinos.

The LSND experiment at the Los Alamos Neutron Scattering Center (LANSCE)<sup>4</sup> is a high-sensitivity search for  $\bar{\nu}_\mu \rightarrow \bar{\nu}_e$  oscillations from  $\mu^+$  decay at rest. With its 1-mA proton intensity and 800-MeV energy, LANSCE is an intense source of low-energy neutrinos. The LANSCE neutrino source is well understood<sup>5,6</sup> because almost all neutrinos arise from  $\pi^+$  or  $\mu^+$  decay;  $\pi^-$  and  $\mu^-$  are readily captured in the iron of the shielding and the copper of the beam stop. The

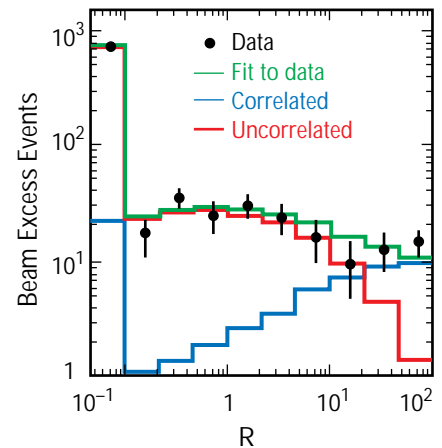


Fig. II-50. An interior view of the LSND detector, showing a portion of the 1,220 phototubes that cover the inside surface.

production of kaons and heavier mesons is negligible at the 800-MeV LANSCE energy. In the 36- to 52.8-MeV energy range, the ratio of  $\bar{\nu}_e$  to  $\bar{\nu}_\mu$  is calculated to be only  $4 \times 10^{-4}$ , so the observation of a significant  $\bar{\nu}_e$  rate would be evidence for  $\bar{\nu}_\mu \rightarrow \bar{\nu}_e$  oscillations.

The LSND detector consists of a cylindrical tank, 8.3 m long by 5.7 m in diameter, surrounded by a veto shield<sup>7</sup> that detects cosmic-ray muons going through the detector. The center of the detector is 30 m from the neutrino source. Mounted on the inside surface of the tank are 1,220 Hamamatsu phototubes (8 in. each), which cover 25% of the surface. These phototubes can be seen in Fig. II-50, a photograph of the inside of the LSND detector. The tank is filled with 167 metric tons of liquid scintillator, which consists of a small concentration of the organic compound butyl PBD in mineral oil. Because of the low scintillator concentration, both Cerenkov light and scintillation light can be detected, and a relatively large attenuation length of more than 20 m occurs for wavelengths greater than 400 nm.<sup>8</sup> A typical 45-MeV electron created in the detector produces approximately 1500 photoelectrons, of which around 280 are in the Cerenkov cone. The phototube time and pulse-height signals are used to reconstruct the electron and positron tracks with an average rms position resolution of  $\sim 30$  cm, an angular resolution of  $\sim 12^\circ$ , and an energy resolution of  $\sim 7\%$ . The Cerenkov cone for relativistic particles and the time distribution of the light (broader for nonrelativistic than for relativistic particles) provide excellent particle identification.

The signature for a  $\bar{\nu}_e$  interaction in the detector is the reaction  $\bar{\nu}_e p \rightarrow e^+ n$ . The recoil neutron,  $n$ , then undergoes the reaction  $np \rightarrow d\gamma$ , in which  $\gamma$  is a correlated 2.2-MeV photon. To distinguish between a correlated photon and a photon that is accidentally coincidental, we use a likelihood ratio,  $R$ , which is the probability that the photon is correlated divided by the probability that it is accidental. The ratio depends on the number of phototubes that the photons have hit, the reconstructed distance between the photon and the positron, and the relative time between the photon and the positron. Figure II-51 shows the  $R$  distribution for events with positrons in the energy range of 20–60 MeV, where an event is defined as the primary positron and any associated photons. The  $R$  distribution yields a range of 26.9–78.5 excess events after beam-off background is subtracted from beam-on readings; this range includes statistical and systematic errors. If these excess events are due to neutrino oscillations, then the oscillation probability, including statistical and systematic errors, is in the range of 0.14%–0.43%. With such a small probability, it is not surprising that neutrino oscillations are difficult to detect.



**Fig. II-51.** The  $R$  distribution for events with positron energies in the range of 20–60 MeV. Shown are the total fit to the data (green), the component of the fit with uncorrelated photons (red), and the component with correlated photons (blue). High values of  $R$  indicate a high probability that a photon is correlated.

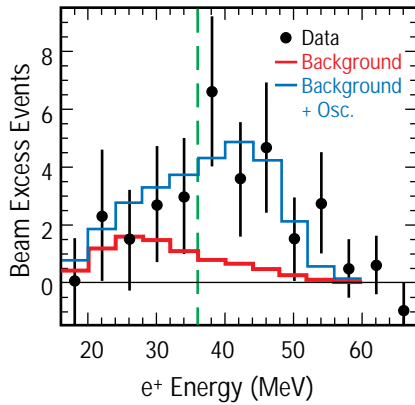


**Fig. II-52.** The positron energy distribution for events with  $R > 30$ . Shown are the beam-excess data, estimated background from all neutrino reactions (red), and neutrino background plus the expected distribution for neutrino oscillations at asymptotically large  $\Delta m^2$  (blue).

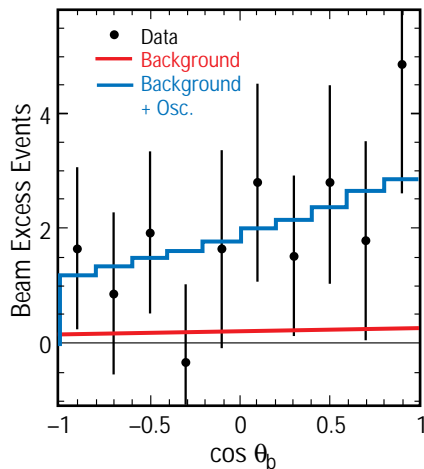


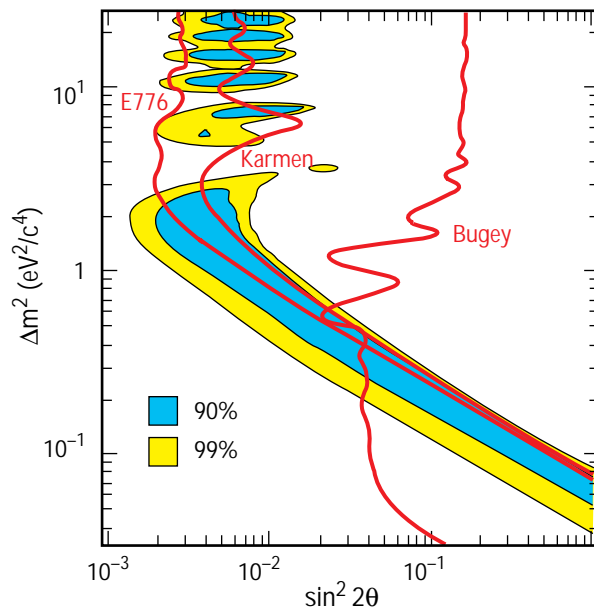
**Fig. II-53.** The angular distribution for events with  $R > 30$ , where  $\theta_b$  is the angle between the positron direction and incident neutrino direction.

**Fig. II-54.** The 90% and 99% likelihood regions of  $\Delta m^2$  vs  $\sin^2 2\theta$  for the LSND experiment, including systematic errors. Also shown are the 90% confidence level limits from KARMEN at ISIS, E776 at BNL, and Bugey reactor experiments; their 90% likelihood regions lie to the left of the limits.

Figures II-52 and II-53 show the positron energy and angular distributions (with beam-off background subtracted) for events that have an associated photon with  $R > 30$ . If  $R$  is greater than 30, the total efficiency of detecting 2.2-MeV photons is 23%, and the probability that an event has an accidental photon in coincidence is 0.6%. In the 36- to 60-MeV energy range, a range chosen because it has little background from known neutrino interactions, there are 22 beam-on events and a total estimated background range of 4.0–5.2 events; the total estimated background includes beam-off background and known neutrino-induced interactions. The probability that this excess of beam-on events is a statistical fluctuation is less than  $10^{-7}$ .

If neutrino oscillations cause the observed excess, then Fig. II-54 shows the allowed region (90% and 99% likelihood regions) of  $\sin^2 2\theta$  plotted against  $\Delta m^2$ . This plot is a maximum likelihood fit to the excess events, where  $\theta$  is the mixing angle and  $\Delta m^2$  is the difference between the squared masses of the two neutrino mass eigenstates. For this plot to have meaning, neutrinos must have mass, and furthermore, different flavors of neutrinos must have different masses. Also shown in Fig. II-54 are the 90% confidence limits from the ongoing KARMEN neutrino experiment at the spallation neutron source ISIS,<sup>9-11</sup> the E776 experiment at Brookhaven National Laboratory,<sup>12</sup> and the Bugey reactor experiment.<sup>13</sup> To the left of these limits are the 90% likelihood regions. If we consider the regions from all four experiments, the most favored region has a  $\Delta m^2$  of approximately  $0.2\text{--}2 \text{ eV}^2/c^4$ .

By acquiring additional data from the experiment and studying the performance of the LSND detector, we expect to improve our understanding of the phenomena described in this article, and we hope eventually to settle the issue of whether neutrino oscillations exist.



## References

1. C. Athanassopoulos et al., "Candidate Events in a Search for  $\bar{\nu}_\mu \rightarrow \bar{\nu}_e$  Oscillations," *Physical Review Letters* **75**, 2650 (1995).
2. C. Athanassopoulos et al., "Evidence for  $\bar{\nu}_\mu \rightarrow \bar{\nu}_e$  Oscillations from the LSND Experiment at the Los Alamos Meson Physics Facility," *Physical Review Letters* **77**, 3082 (1996).
3. C. Athanassopoulos et al., "Evidence for Neutrino Oscillations from Muon Decay at Rest," *Physical Review C* **54**, 2685 (1996).
4. C. Athanassopoulos et al., "The Liquid Scintillator Neutrino Detector and LAMPF Neutrino Source," *Nuclear Instruments and Methods in Physics Research A* **388**, 149 (1997).
5. R. L. Burman, M. E. Potter, and E. S. Smith, "Monte Carlo Simulation of Neutrino Production by Medium-Energy Protons in a Beam Stop," *Nuclear Instruments and Methods in Physics Research A* **291**, 621 (1990).
6. R. L. Burman, A. C. Dodd, and P. Plischke, "Neutrino Flux Calculations for the ISIS Spallation Neutron Facility," *Nuclear Instruments and Methods in Physics Research A* **368**, 416 (1996).
7. J. J. Napolitano et al., "Construction and Performance of a Large Area Scintillator Cosmic Ray Anticoincidence Detector," *Nuclear Instruments and Methods in Physics Research A* **274**, 152 (1989).
8. R. A. Reeder et al., "Dilute Scintillators for Large-Volume Tracking Detectors," *Nuclear Instruments and Methods in Physics Research A* **334**, 353 (1993).
9. B. Bodmann et al. (KARMEN Collaboration), "First Observation of the Neutral Current Excitation  $^{12}\text{C}(\nu, \nu')^{12}\text{C}^*(1^+, 1)$ ," *Physics Letters B* **267**, 321 (1991).
10. B. Bodmann et al. (KARMEN Collaboration), "Cross Section of the Charged Current Reaction  $^{12}\text{C}(\nu_e, e^-)^{12}\text{N}_{\text{g.s.}}$ ," *Physics Letters B* **280**, 198 (1992).
11. B. Zeitnitz et al. (KARMEN Collaboration), "KARMEN: Neutrino Physics at ISIS," *Progress in Particle and Nuclear Physics* **32**, 351 (1994).
12. L. Borodovsky et al., "Search for Muon-Neutrino Oscillations  $\nu_\mu \rightarrow \nu_e$  ( $\bar{\nu}_\mu \rightarrow \bar{\nu}_e$ ) in a Wide-Band Neutrino Beam," *Physical Review Letters* **68**, 274 (1992).
13. B. Achkar et al., "Search for Neutrino Oscillations at 15, 40, and 95 Meters from a Nuclear Power Reactor at Bugey," *Nuclear Physics B* **434**, 503 (1995).